Journal of Mathematical Chemistry 10(1992)221–247

CHROMOPHORES IN SPECTROSCOPY: AB INITIO STUDIES OF LOCALIZED DESCRIPTIONS OF MOLECULAR ELECTRONIC EXCITATIONS

Aage E. HANSEN
Department of Physical Chemistry, H.C. Ørsted Institute, Universitetsparken 5, DK-2100 Copenhagen Ø, Denmark

and

Thomas D. BOUMAN
Department of Chemistry, Southern Illinois University, Edwardsville, IL 62026, USA

Abstract

We review a computationally efficient approach, based jointly on the Random Phase Approximation (RPA) and on localized molecular orbitals, for calculating and analyzing electronic excitations in terms of the nature of the chromophore and its interaction with its molecular surroundings. The method is applied to two typical chromophoric systems using ab initio extended-basis calculations: the non-conjugated but electronically coupled ethylenic double bonds in norbornadiene (NBD, bicyclo[2.2.1]hepta-2,5-diene) and the chirally perturbed carbonyl chromophore in *equatorial* 4-methyladamantanone (EMAO). The analyses are a posteriori in nature but provide insights into the spectroscopic properties of medium-sized molecules.

1. Introduction

In a broad sense, the concept of a chromophore, the color-bearing part of a molecule, pervades almost all of molecular spectroscopy, from nuclear magnetic resonance, where a spinning nucleus is the chromophore, to optical spectroscopies where molecular fragments are color-bearers. The history of the concept can be traced to the need for a molecular color theory in the development of synthetic dyes in the last half of the 19th century [1]. In modern terms, the presence of a particular chromophore is revealed by spectral response in one or more characteristic regions for example by the group frequencies that identify vibrational chromophores or the visible and ultraviolet absorption bands that characterize electronic chromophores whereas the exact spectral positions and features such as band shapes, splittings and intensities, serve to identify the molecular environment embedding the chromophore.

From a theoretical point of view, results from ab initio calculations of molecular electronic transitions do not readily reveal the kind of transferability and localization implied in the chromophore concept in electronic spectroscopy. Each molecule is

treated individually, and meaningful analyses into excitation contributions involving its various bonds or fragments are complicated by the inherently delocalized description of the overall excitation process. This arises from including a large number of electronic configurations expressed in terms of delocalized molecular orbitals, which in turn are possibly expanded in basis sets containing diffuse atomic orbitals.

We shall outline and illustrate an approach based on the Random Phase Approximation (RPA) [2–5], where introducing localized occupied molecular orbitals allows a localized analysis as well as various pictorial representations of the excitation process that can serve to identify the chromophore for a particular electronic transition in a given molecule. The localized analysis leads to well-defined bond and fragment contributions, both to the excitation amplitudes and to various intensity measures, and the pictorial representations include charge rearrangements and transition densities as well as effective virtual orbitals. The representations of the effective virtual orbitals provide a useful indication of the local versus charge-transfer nature of the transitions. Our emphasis here is accordingly on employing localized molecular orbitals for the a posteriori analysis of an ab initio calculation, aiming at elucidating the nature of the chromophore and of the extrachromophoric interactions, whereas the construction of transferable chromophoric characteristics will not be pursued per se. In fact, the results suggest that the quantities defined here for the purpose of the analysis are not transferable in general.

Section 2 contains the theoretical background, including an outline of the working equations for the random phase approximation, the general intensity expressions, and the expressions for the quantities designed specifically for the analysis of the nature of the excitations. The results and analyses obtained for the two characteristic molecular systems, bicyclo[2.2.1]hepta-2,5-diene (norbornadiene, NBD) and 4(e)-methyladamantanone (EMAO), are given in section 3. These molecules allow the study of the ethylene and carbonyl chromophores, of the interactions between these chromophores, and of the interactions with the saturated molecular environment. The second of these systems is chiral, and thus exhibits natural circular dichroism spectra in addition to the ordinary absorption spectra. Since natural circular dichroism is particularly sensitive to intramolecular interactions [3], this type of spectral response is included in the present account. Section 4 contains concluding remarks.

Localized molecular orbitals have of course been used extensively in semiempirical as well as ab initio quantum-chemical approaches to molecular electronic properties (see, e.g., ref. [6]). For other recent approaches, including approaches introducing more general localized wave functions, see, e.g., the works of Surján [7] on localized geminals, of Weinhold [8] on natural localized molecular orbitals, of Kirtman [9] on a local space approximation, of Maggiora et al. [10] on approximations in exciton theory, of Petke [11] on local description of chromophores, and of Pulay [12] on local treatments of the correlation energy. We make no pretence of completeness in the above list, which is meant only to be suggestive of the range of activity in this area.

2. Theory

The most important of the quantities characterizing an electronic absorption band are the transition energy and various integrated intensity measures. These quantities are obtainable from linear response calculations based on the electronic ground-state wave function at the equilibrium molecular geometry, and this is the approach we shall outline below. A complete characterization, including shape and width of the absorption band, requires a quantum approach to the full vibronic molecular problem (see, e.g., ref. [3] or [13]) that falls outside the scope of the present paper.

The nature of chromophoric molecular fragments and their interactions with the molecular environment may be studied by considering the ordinary absorption intensity as measured by the oscillator strength f_q, as well as the natural circular dichroic intensity as measured by the rotatory strength R_q, for an electronic excitation $0 \rightarrow q$ [3]. Among various equivalent expressions for these intensities are the following (using atomic units throughout) [3]:

$$f_q^{r\nabla} = (2/3)\langle 0|\nabla|q\rangle \cdot \langle 0|\mathbf{r}|q\rangle \tag{1}$$

and

$$R_q^{\nabla} = (2c\omega_q)^{-1}\langle 0|\nabla|q\rangle \cdot \langle 0|\mathbf{r}\times\nabla|q\rangle, \tag{2}$$

where $\langle 0|\nabla|q\rangle$ and $\langle 0|\mathbf{r}|q\rangle$ are, respectively, the velocity and length versions of the electric dipole transition moment, and $\langle 0|\mathbf{r}\times\nabla|q\rangle/2c$ is (the imaginary part of) the magnetic dipole transition moment for the qth excitation. The transition energy is ω_q, and c is the speed of light. Other expressions follow by application of the relation

$$\langle 0|\nabla|q\rangle = \langle 0|[\mathbf{r}, H]|q\rangle = \omega_q\langle 0|\mathbf{r}|q\rangle, \tag{3}$$

which is the most widely used special case of the hypervirial relation

$$\langle 0|[F, H]|q\rangle = \omega_q\langle 0|F|q\rangle \tag{4}$$

involving the commutator between an arbitrary operator and the Hamiltonian.

2.1. THE RANDOM PHASE APPROXIMATION

We restrict our considerations to molecules with a ground state described sufficiently well by a closed-shell Hartree–Fock wave function. The RPA then provides the correct linear response approach, yielding the transition moments and energies appearing in eqs. (1) and (2) through first order in electron correlation [2, 14, 15]. Qualitatively speaking, the RPA works as well for the transition energies and intensities as the Hartree–Fock approximation itself works for the ground state

Specifically, in the RPA the transition moment for a spin-free one-electron operator can be written as

$$\langle 0|\hat{A}|q\rangle = 2^{1/2}\sum_{\alpha m}\{\langle\alpha|\hat{A}|m\rangle X_{\alpha m,q} + \langle m|\hat{A}|\alpha\rangle Y_{\alpha m,q}\}, \tag{5}$$

where α denotes a molecular orbital (MO) occupied in the Hartree–Fock ground state, and m denotes a virtual orbital; the factor of $2^{1/2}$ arises from adaptation to spin-singlet excitations. The amplitudes $X_{\alpha m,q}$ and $Y_{\alpha m,q}$, together with the excitation energies ω_q, are determined in the RPA by the set of coupled linear equations

$$\sum_{\beta n}\{A_{\alpha m,\beta m}X_{\beta n,q} + B_{\alpha m,\beta n}Y_{\beta n,q}\} = \omega_q X_{\alpha m,q}, \tag{6a}$$

$$\sum_{\beta n}\{B_{\alpha m,\beta n}X_{\beta n,q} + A_{\alpha m,\beta n}Y_{\beta n,q}\} = -\omega_q Y_{\alpha m,q}. \tag{6b}$$

The elements of the **A** and **B** matrices are

$$\begin{aligned} A_{\alpha m,\beta n} &= \langle \alpha \to m|H - E_0|\beta \to n\rangle \\ &= F_{mn}\delta_{\alpha\beta} - F_{\alpha\beta}\delta_{mn} + [1 + (-1)^S](m\alpha|\beta n) - (mn|\alpha\beta), \end{aligned} \tag{7a}$$

$$\begin{aligned} B_{\alpha m,\beta n} &= \langle \alpha \to m, \beta \to n|H|\Delta_0\rangle \\ &= (m\alpha|n\beta) + (-1)^S[(m\alpha|n\beta) - (n\alpha|\beta n)], \end{aligned} \tag{7b}$$

where S is the spin quantum number (0 or 1), $|\Delta_0\rangle$ is the Hartree–Fock ground-state wave function, F_{ij} is an MO matrix element of the Fock operator, and $(ij|kl)$ is a two-electron repulsion integral in the Mulliken notation [15,16]. The rows and columns of **A** and **B** are indexed by the set of singly-excited configurations $|\alpha \to m\rangle$. Inclusion of doubly-excited configurations through the **B** matrix ensures consistent first-order treatment of electron correlation for the response properties. A second-quantized derivation of the RPA is given in ref. [2]; for a first-quantized derivation, see ref. [14]. For the transition moments appearing in the intensities, eqs. (1) and (2), eq. (5) specializes to

$$\langle 0|\mathbf{r}|q\rangle = 2^{1/2}\sum_{\alpha}\sum_{m}\langle\alpha|\mathbf{r}|m\rangle(X_{\alpha m,q} + Y_{\alpha m,q}), \tag{8a}$$

$$\langle 0|\nabla|q\rangle = 2^{1/2}\sum_{\alpha}\sum_{m}\langle\alpha|\nabla|m\rangle(X_{\alpha m,q} - Y_{\alpha m,q}), \tag{8b}$$

$$\langle 0|\mathbf{r}\times\nabla|q\rangle = 2^{1/2}\sum_{\alpha}\sum_{m}\langle\alpha|\mathbf{r}\times\nabla|m\rangle(X_{\alpha m,q} - Y_{\alpha m,q}), \tag{8c}$$

utilizing the Hermitian and anti-Hermitian character of the respective operators.

The RPA excitation amplitudes are normalized in the sense

$$\sum_{\alpha m}(X^2_{\alpha m,q} - Y^2_{\alpha m,q}) \equiv \sum_{\alpha m} w_{\alpha m,q} = 1, \tag{9}$$

and although RPA theory does not directly yield excited-state properties, the following prescription for the difference in expectation values of one-electron operators $\hat{A}$ between an RPA excited "state" and the ground state affords an indirect route to these properties [17]:

$$\langle q|\hat{A}|q\rangle - \langle 0|\hat{A}|0\rangle = \Delta_{0,q}(\hat{A})$$
$$= \sum_{\alpha m}\sum_{\beta n}\{\langle m|\hat{A}|n\rangle\delta_{\alpha\beta} - \langle \alpha|\hat{A}|\beta\rangle\delta_{mn}\}\Xi^q_{\alpha m,\beta n}, \tag{10}$$

where

$$\Xi^q_{\alpha m,\beta n} = X^*_{\alpha m,q}X_{\beta n,q} + Y^*_{\alpha m,q}Y_{\beta n,q}. \tag{11}$$

For $\hat{A}$ equal to the one-electron density operator $\delta(\boldsymbol{r}-\boldsymbol{r}')$, eq. (10) provides the charge rearrangement density [18]

$$\Delta_{0,q}(\mathbf{r}) = \sum_{\alpha m}\sum_{\beta n}\{\phi^*_m(\mathbf{r})\phi_n(\mathbf{r})\delta_{\alpha\beta} - \phi^*_\alpha(\mathbf{r})\phi_\beta(\mathbf{r})\delta_{mn}\}\Xi^q_{\alpha m,\beta n}, \tag{12}$$

which can be analyzed or plotted to visualize the difference in charge distribution brought about by the excitation. For $\hat{A} = -e\mathbf{r}$, eq. (10) yields the dipole moment difference between states $|q\rangle$ and $|0\rangle$, and for $\hat{A} = x^2$, y^2, or z^2, the changes in extent of the charge distribution give a direct indication of the valence or Rydberg nature of the excitation.

A different indicator of the nature of an electronic excitation is obtained by noting that the dipole length transition moment may be expressed in terms of a transition density through the relation

$$\langle 0|\mathbf{r}|q\rangle = \int dV\, \mathbf{r}\,\rho_{0,q}(\mathbf{r}), \tag{13}$$

for which eq. (8a) yields the transition density [18]

$$\rho_{0,q}(\mathbf{r}) = 2^{1/2}\sum_{\alpha}\sum_{m}\phi^*_\alpha(\mathbf{r})\phi_m(\mathbf{r})(X_{\alpha m,q} + Y_{\alpha m,q}). \tag{14}$$

Plots or analyses of this transition density indicate the source of the electric dipole intensity of the excitation. The difference in the nature of the densities given in eqs. (12) and (14) is discussed in ref. [18].

The attractive formal properties of the RPA include the fulfillment, in a complete Hartree–Fock basis, of the hypervirial relation, eq. (4), for a general one-

electron operator $\hat{A}$. As a consequence, the RPA guarantees the equivalence (in a complete Hartree–Fock basis) of length and velocity forms of electronic transitions moments, i.e. eq. (3), and the fulfillment of intensity sum rules [3]. The RPA is size-consistent, and as demonstrated elsewhere [16], it is invariant to arbitrary unitary transformations within occupied and virtual orbital sets, which allows the use of localized MOs. The latter feature is essential in analyzing chromophoric character, as mentioned in the introduction and further discussed below. It is anticipated in eq. (7a) by the appearance of a general (off-diagonal) representation of the Fock operator. For canonical orbitals, $F_{mn} = \varepsilon_m \delta_{mn}$ and $F_{\alpha\beta} = \varepsilon_\alpha \delta_{\alpha\beta}$, where ε_m and ε_α are orbital energies.

2.2. LOCALIZED ANALYSIS OF EXCITATIONS AND INTENSITIES

Present implementations of the RPA method presuppose solving the Hartree–Fock equations to provide the sets of occupied and virtual canonical MOs. For decomposing the optical properties into chromophoric contributions, or more generally into bond or fragment contributions, we base our approach on the Foster–Boys procedure for constructing localized occupied MOs [16,19]. However, the Foster–Boys method characteristically produces "banana" bonds for multiple bonds, Kekulé-type structures with banana bonds for most benzenoid aromatics, and essentially sp^2-hybridized orbitals for double lone pairs such as those in ketones. To retain the often more attractive notion of contributions from sigma and pi orbitals, and from C_{2v}-adapted non-bonding orbitals in carbonyl groups, we can utilize the freedom to choose whatever unitary transformation we want among the occupied orbitals [5,16]. Thus, we can either apply the Foster–Boys procedure selectively within groups of orbitals, for example for benzenoid aromatics by localizing the heavy-atom core orbitals and the orbitals in the σ framework separately, leaving the π orbitals delocalized, or apply a selective redelocalization subsequent to the Foster–Boys localization [20]. The latter procedure generates local σ and π orbitals for isolated double bonds and conventional non-bonding type orbitals in ketones by diagonalization within the particular block, or blocks, of the non-canonical Fock matrix connecting the pertinent localized orbitals. An example is the 2×2 block connecting the banana orbitals in a double bond. If localization of the virtual orbitals is desired, we employ a procedure based on maximizing the sum of the dipole strengths of excitations out of the occupied localized orbitals into (normally a subset of) the virtual orbitals [20]. If only a subset of the virtual orbitals is localized, the remaining virtual orbitals are "symmetry-adapted" by diagonalizing the Fock matrix within this orthogonal complement space. However, for most of the quantities discussed below, localization of the virtual orbitals is immaterial.

Assuming now that the occupied orbitals are localized according to one of the procedures outlined above, the quantity $w_{\alpha m}$ defined in eq. (9) represents the weight of the individual orbital promotion $\alpha \rightarrow m$ in the composition of excitation

$0 \rightarrow q$, and hence the total weight with which bond α contributes to the normalization of this excitation, is given by

$$w_{\alpha,q} = \sum_m w_{\alpha m,q}, \tag{15}$$

where m is summed over all the virtual orbitals. For simplicity, we use the term "bond" to refer to any localized occupied orbital, including core, bonding, or non-bonding orbitals. $w_{\alpha,q}$ can of course be further summed over a group of bonds to yield the total normalization contribution for a fragment or chromophore.

In a similar vein, based on eq. (8) we can define the following bond transition moments:

$$\mathbf{r}_{\alpha,q} = 2^{1/2} \sum_m \langle \alpha | \mathbf{r} | m \rangle (X_{\alpha m,q} + Y_{\alpha m,q}), \tag{16}$$

$$\mathbf{p}_{\alpha,q} = 2^{1/2} \sum_m \langle \alpha | \nabla | m \rangle (X_{\alpha m,q} - Y_{\alpha m,q}), \tag{17}$$

$$\begin{aligned} \boldsymbol{\ell}_{\alpha,q} &= 2^{1/2} \sum_m \langle \alpha | \mathbf{r} \times \nabla | m \rangle (X_{\alpha m,q} - Y_{\alpha m,q}) \\ &= \boldsymbol{\ell}'_{\alpha,q} + \rho_\alpha \times \mathbf{p}_{\alpha,q}, \end{aligned} \tag{18}$$

with

$$\boldsymbol{\ell}'_{\alpha,q} = 2^{1/2} \sum_m \langle \alpha | (\mathbf{r} - \rho_\alpha) \times \nabla | m \rangle (X_{\alpha m,q} - Y_{\alpha m,q}), \tag{19}$$

where

$$\rho_\alpha = \langle \alpha | \mathbf{r} | \alpha \rangle \tag{20}$$

is the centroid of bond orbital α, and where the index m is again summed over all the virtual orbitals. These bond moments therefore represent the contributions to a particular total transition moment due to excitations out of the individual localized bond orbitals. Here, $\boldsymbol{\ell}'_{\alpha,q}$ of eq. (19) specifically represents the local magnetic dipole transition moment for excitations out of orbital α with the origin for the magnetic dipole moment operator at the centroid for this orbital. The reason for the manipulation of the angular momentum matrix elements in eq. (18) is that $\boldsymbol{\ell}_{a,q}$ itself is not physically meaningful, since its magnitude and direction in general depends on the arbitrary choice of the overall molecular coordinate system, as is apparent in eq. (18). On the other hand, $\boldsymbol{\ell}'_{\alpha,q}$ can be identified as an inherent magnetic dipole transition moment contribution associated with bond α [18].

These bond moments can be employed in eqs. (8) and subsequently in eqs. (1) and (2) to yield

$$f_q = (2/3)\sum_{\alpha} \mathbf{p}_{\alpha,q} \cdot \mathbf{r}_{\alpha,q}$$

$$+ (1/3) \sum_{\alpha \neq \beta} (\mathbf{p}_{\alpha,q} \cdot \mathbf{r}_{\beta,q} + \mathbf{p}_{\beta,q} \cdot \mathbf{r}_{\alpha,q}) \equiv \sum_{\alpha,\beta} f^q_{\alpha,\beta} \tag{21}$$

and

$$R_q = (2c\omega_q)^{-1} \sum_{\alpha} \mathbf{p}_{\alpha,q} \cdot \boldsymbol{\ell}'_{\alpha,q} + (2c\omega_q)^{-1} \sum_{\alpha \neq \beta} \mathbf{p}_{\alpha,q} \cdot \boldsymbol{\ell}'_{\beta,q}$$

$$+ (4c\omega_q)^{-1} \sum_{\alpha \neq \beta} (\rho_a - \rho_b) \cdot (\mathbf{p}_{\alpha,q} \times \mathbf{p}_{\beta,q}) \tag{22a}$$

$$\equiv \sum_{\alpha,\beta} R^q_{\alpha,\beta} \tag{22b}$$

for the two intensities. In eq. (21), the second term is symmetrized in the bond indices α and β to give equal weight to the length and velocity bond contributions in the oscillator strength. The three distinct terms in the expression for the rotatory strength, eq. (22a), can be identified with the three mechanisms for natural optical rotatory power contained in Kirkwood's theory [3,18,21], and can be labelled intrinsic, $\mu-m$ [22], and polarizability ("$\mu-\mu$") contributions, respectively. The intrinsic terms reflect chiral distortions of the individual bonds, the $\mu-m$ terms measure the contributions from couplings between local electric and magnetic dipole transition moments in separate bonds, and the polarizability terms measure the "moment-of-momentum" type contributions from coupling between local electric dipole transition moments.

In addition to this mechanistic analysis of the rotatory strength, the intensity expressions in eqs. (21) and (22) provide explicit decompositions into bond contributions (summation over α only) and bond–bond contributions (summation over $\alpha \neq \beta$). This allows identification of the bonds or fragments dominating the respective intensities, i.e., the chromophore or chromophores for a given excitation. For some purposes, the analyses expressed by eqs. (21) and (22) are too detailed to be useful and more coarse-grained pictures can be obtained by introducing effective bond contributions defined as

$$f^q = \sum_{\alpha} [f^q_{\alpha\alpha} + 1/2 \sum_{\beta}{}' (f^q_{\alpha\beta} + f^q_{\beta\alpha})] \equiv \sum_{\alpha} f^q_{\alpha,\mathrm{eff}}, \tag{23}$$

$$R^q = \sum_{\alpha} [R^q_{\alpha\alpha} + 1/2 \sum_{\beta}{}' (R^q_{\alpha\beta} + R^q_{\beta\alpha})] \equiv \sum_{\alpha} R^q_{\alpha,\mathrm{eff}}. \tag{24}$$

If desired, effective bond contributions to the three distinct rotatory strength mechanisms can be obtained from eq. (24), *mutatis mutandis*.

The summation over all virtual orbitals in the various bond contributions defined in eqs. (15)–(19) makes it immaterial whether the virtual orbitals are localized. However, at the same time this feature obliterates a number of details in the description of the excitations, such as distinctions between local and charge-transfer excitations and between degenerate and non-degenerate exciton couplings. Some indication of these features can be gleaned from the individual normalization contributions $w_{\alpha m,q}$ of eq. (9), if the virtual orbitals are localized. More informative representations of the nature of the excitations can be obtained from population analyses or contour plots of charge rearrangements, eq. (12), and transition densities, eq. (14), or from changes in the effective size of the electron distribution as discussed in connection with eqs. (10)–(12). As we shall illustrate below, the question of the local versus charge-transfer nature of the intensity contributions from excitations of the individual bonds can be studied either by population analyses or by contour plots of the excitation-specific effective virtual orbitals, which are defined as

$$EVO_{\alpha}^{q}(\mathbf{r}) = \sum_{m} \phi_m(\mathbf{r})\,(X_{\alpha m,q} + Y_{\alpha m,q}), \tag{25}$$

in accord with the definition of the transition density, eq. (14).

We emphasize that the decompositions into bond contributions to normalization, transition moments, and intensities, eqs. (15), (16)–(19) and (21)–(24), and the definition of the effective virtual orbitals, eq. (25), do not involve any additional approximations over and above those entering the RPA method itself.

The above-mentioned invariance of the RPA method with respect to separate unitary transformations within the occupied and the virtual orbital spaces implies that the calculations can be carried out in two ways. Either one can use localized MOs throughout, i.e., solving the RPA equations using the non-canonical version given in eqs. (7) and employing the resulting amplitudes $(X \pm Y)$ directly in the subsequent intensity calculations and analyses, or one can execute the RPA calculations in a canonical MO basis and subsequently transform the amplitudes and the intensities into localized basis representations as discussed in ref. [16]. For molecules and basis sets of the size considered here, the RPA equations are normally solved by iterative procedures [5,23], which converge considerably faster in canonical bases than in localized bases, so that the second strategy is generally preferred.

3. Chromophore case studies

3.1. NORBORNADIENE

The molecule bicyclo[2.2.1]hepta-2,5-diene (norbornadiene, NBD) contains two equivalent, non-conjugated ethylenic groups and exhibits C_{2v} symmetry (see fig. 1 for molecular skeleton, atomic numbering and coordinate system). The present consensus concerning the experimental photoelectron and optical spectra as summarized and assigned by Doering and McDiarmid [24] is included in table 1. In addition to

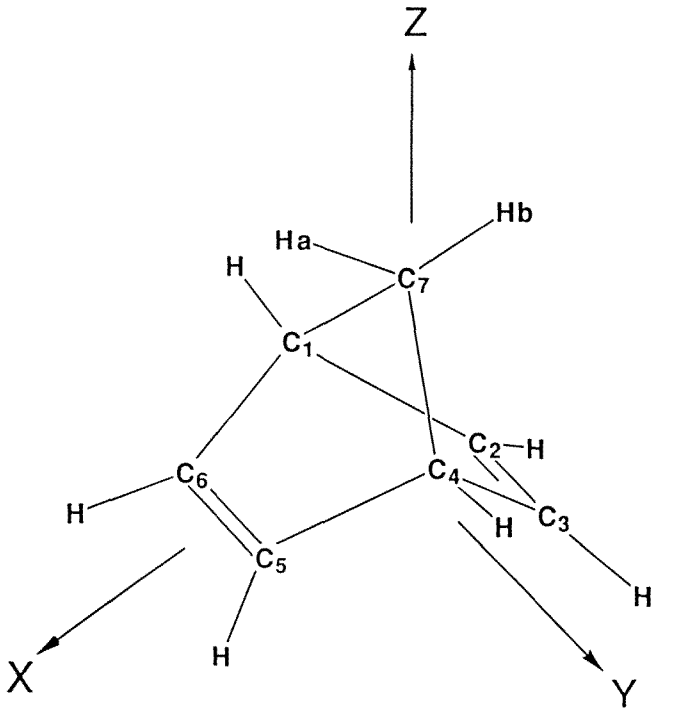

Fig. 1. Atom numbering scheme and coordinate system for norbornadiene.

Table 1

Low-lying singlet excitations in norbornadiene.

ΔE [eV]		$f^{r\nabla}$	$\Delta\langle r^2\rangle$[a]	Assignments			
Calc.	Exp.[b]		[a.u.]	Present	%LE[c]	%CT[c]	Doering and McDiarmid[b]
5.28	5.25	0.00	7.7	A_2 exciton−	55	25	$\pi_2 \rightarrow \pi_3$
6.34	5.95	0.02	51.0	$B_1\ \pi_2 \rightarrow 3s$	0	0	$\pi_2 \rightarrow 3s$
6.70	6.65	0.02	57.4	$A_1\ \pi_2 \rightarrow 3p_x$	0	0	$\pi_2 \rightarrow 3p$
6.99	5.95	0.20	12.2	B_2 exciton+	45	10	$\pi_1 \rightarrow \pi_3$
	6.65						$\pi_2 \rightarrow \pi_4$
7.01		0.00	48.0	$A_2\ \pi_2 \rightarrow 3p_y$	5	0	
7.14		0.01	28.8	$B_1\ \pi_2 \rightarrow 3p_z$	0	0	
	6.85						$\pi_1 \rightarrow 3s$
7.16	7.18	0.03	34.0	$B_2\ \pi_2 \rightarrow 3d_{xy}$	5	20	$\pi_2 \rightarrow 3d$

[a] Calculated from eq. (10) with $A = r^2$.
[b] Ref. [24].
[c] See text.

a number of Rydberg-like transitions, this assignment claims the presence of three valence-like transitions in the region considered, namely an electric-dipole-forbidden–magnetic-dipole-allowed transition at 5.25 eV, as supported also by circular dichroism results for chirally substituted norbornadienes [25], and electric-dipole-allowed transitions at about 5.95 eV and 6.65 eV, each of the latter two overlapping a Rydberg-like transition.

Early theoretical treatments were based on delocalized π-electron models [26], through-bond, through-space interactions [27], and molecular exciton interactions [1]. Minimal basis set RPA calculations have been presented for substituted norbornadienes [25]. After completion of the present work, RPA calculations on a number of dienes, including NBD, were reported by Galasso [28]; these calculations are however not fully ab initio, since experimental ionization potentials are used in place of calculated energies for the valence orbitals. In an exciton description [1], the 5.25 eV and (presumably) the 5.95 eV transitions are interpreted as, respectively, the out-of-phase and the in-phase coupling of local excitations in the ethylene chromophores, whereas Doering and McDiarmid's assignments shown in table 1 are based on the delocalized π-electron description. An attempt to assess the relative validity of the two descriptions was presented in the context of the above-mentioned minimal basis set RPA calculations [25], where it was concluded that the two lowest valence transitions could be classified as, respectively, 70% and 60% locally excited, with about 20% admixture of interchromophoric charge transfer in both transitions. This point will play an essential role in the present treatment.

The norbornadiene calculations presented here were performed on a Silicon Graphics 4D/310S Computer. The molecular orbitals were generated using the Gaussian 90 program [29], and the electronic excitation properties were computed with Program RPAC [30]. We used a force-field (MMX) optimized geometry [31], and a basis set consisting of 107 atomic orbitals: a Dunning–Hay (3s2p) set [32] plus a single set of diffuse s and p functions ($\alpha_s = 0.023$, $\alpha_p = 0.021$) for the carbon atoms and STO-5G for the hydrogen atoms. This yielded a Hartree–Fock ground-state energy of -269.540983 hartrees, and the basis set generated a total of 1476 singly-excited configurations out of the valence occupied orbitals. The effects of double excitations (roughly the square of the number of single excitations) are included through the **B** matrix. All of these were included in the iterative solution of the RPA equations [30], and the overall results for the lowest excitations are given in table 1, where B_1, B_2, and A_1 transform as x, y, and z, respectively, in the molecular coordinate frame indicated in fig. 1. The predicted electric dipole polarizations are hence uniquely defined by the symmetry assignments. The lowest A_2 transition is found to have a large z-polarized magnetic dipole transition moment, whereas the magnetic dipole transition moment of the second A_2 transition is very small.

In more detail, the calculations produce two predominantly valence-like excitations, at 5.28 eV and 6.99 eV, with symmetry and intensity properties in accord with the exciton model, and a number of Rydberg-like excitations, of which we show the lowest five in table 1. The immediate basis for the valence-like or

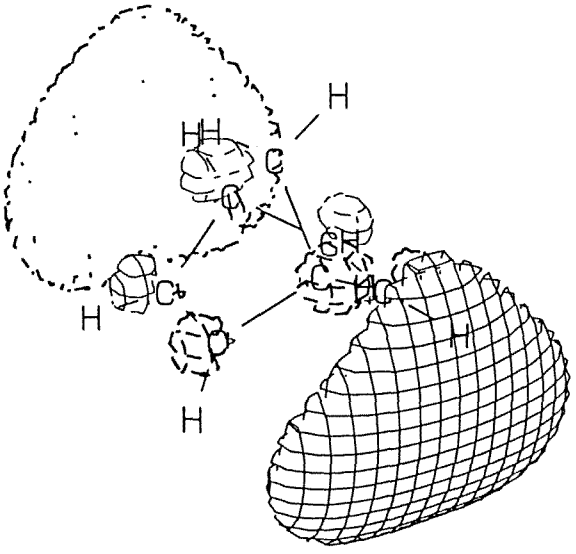

Fig. 2. Contour plot of the $3p_y$ virtual orbital for norbornadiene. All plots are generated using the Jorgensen–Salem algorithms [33]. Solid contours represent positive phase, dashed contours represent negative phase.

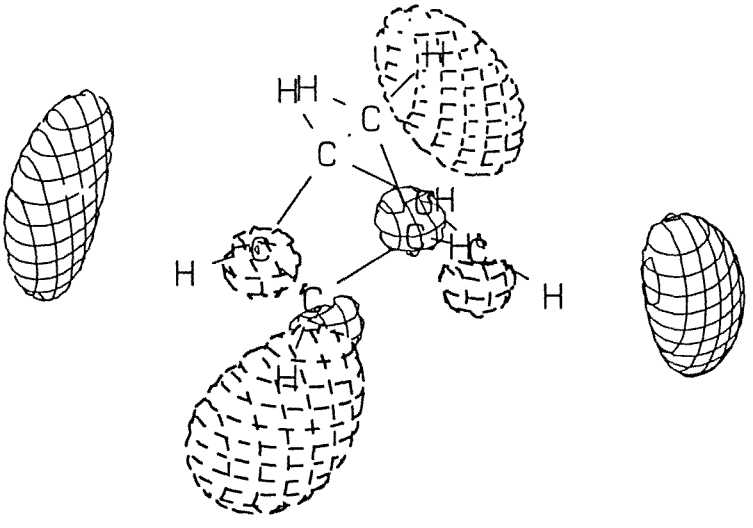

Fig. 3. Contour plot of the $3d_{xy}$ virtual orbital for norbornadiene.

Rydberg-like classification of these excitations is provided by the $\Delta\langle r^2\rangle$ values given in the table, showing that the 5.28 eV and 6.99 eV excitations are much more compact than the excitations classified as Rydbergs. The orbital assignments for the

five Rydberg transitions in the table refer to the canonical MO basis, with π_2 transforming as b_1. The particular single orbital excitation listed for each of these transitions accounts for at least 70% of the normalization (see eq. (9)). The Rydberg orbital characters, 3s, 3p, and 3d, are assigned from the calculated symmetry properties and from inspection of plots of the pertinent (canonical) virtual orbitals. Figures 2 and 3 show the virtual orbitals designated $3p_y$ and $3d_{xy}$ in table 1; the alleged Rydberg character is quite apparent for these orbitals. For the Rydberg excitations, the agreement between calculated and experimental energies and assignments is reasonably good. We elect to leave open the question of whether our computed $\pi_2 \rightarrow 3p_z$ at 7.14 eV should be identified with the experimental 6.85 eV transition assigned as $\pi_1 \rightarrow 3s$ by Doering and McDiarmid. However, we note that the calculations show no Rydberg transitions with predominant excitation out of π_1 within the lowest ten transitions.

For the valence-like transitions, the agreement for the lowest transition is excellent, while for the higher valence-like transitions the most immediate choice, as shown in table 1, is to identify the excitation calculated at 6.99 eV with the valence-like component assigned to the composite experimental band at 5.95 eV. One accepts thereby an error of about 1 eV in the calculated energy of this transition. Using a combined criterion of $\Delta\langle r^2\rangle$ and electric dipole intensity, we find no clear candidate for the second B_2 valence-like transition, experimentally assigned to the 6.65 eV composite band, below 9 eV in the present calculations. A number of excitations in the range 8–9 eV have significant $\pi \rightarrow \pi^*$ contributions, but show little intensity and their $\Delta\langle r^2\rangle$ values are large (about 40–50 au^2). However, a clearly valence-like B_2 transition, $\Delta\langle r^2\rangle = 6.7$ au^2, of $\sigma \rightarrow \pi^*$ character appears at 9.54 eV. In accord with its $\sigma \rightarrow \pi^*$ character, this transition has a large magnetic dipole transition moment, but an almost vanishing electric dipole intensity. The results obtained by Galasso [28] are generally quite similar; in particular, neither calculation locates a $\pi \rightarrow \pi^*$ dominated excitation below 8–8.5 eV that can be correlated with the experimental 6.65 eV feature. The differences between the present results and those reported by Galasso probably stem from the introduction of experimental ionization potentials in Galasso's modified RPA procedure.

Turning now to analyzing the results for the two valence-like transitions calculated at 5.28 eV and 6.99 eV, figs. 4 and 5 show contour plots of the charge rearrangement densities, eq. (12), while figs. 6 and 7 show contour plots for the transition densities, eq. (14), for these transitions. For the A_2 transition, the charge rearrangement is quite localized in the diene moiety (fig. 4), apart from some participation of the bridgehead carbon. The charge rearrangement for the B_2 transition (fig. 5) shows a considerably larger involvement of the entire molecule, in accord with the somewhat larger value for $\Delta\langle r^2\rangle$ for this transition (table 1). The transition densities shown in figs. 6 and 7 both show large contributions in the chromophoric region with some participation of the intervening carbon atoms. However, the important difference here is that the electric dipole forbidden nature of the A_2 transition comes across clearly in the quadrupolar nature of the transition density

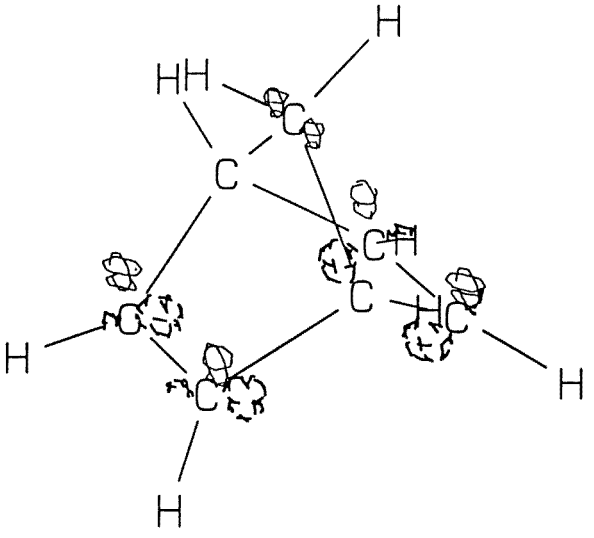

Fig. 4. Contour plot of the charge rearrangement density, eq. (12), for the lowest singlet excitation in norbornadiene.

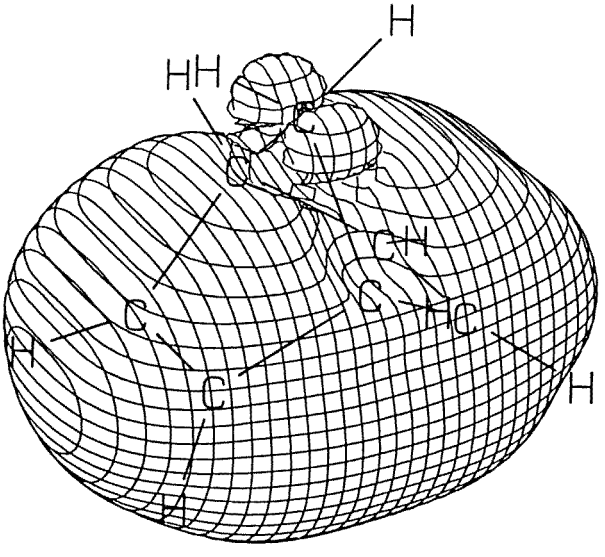

Fig. 5. Contour plot of the charge rearrangement density, eq. (12), for the fourth singlet exctation in norbornadiene, on the same scale as fig. 4.

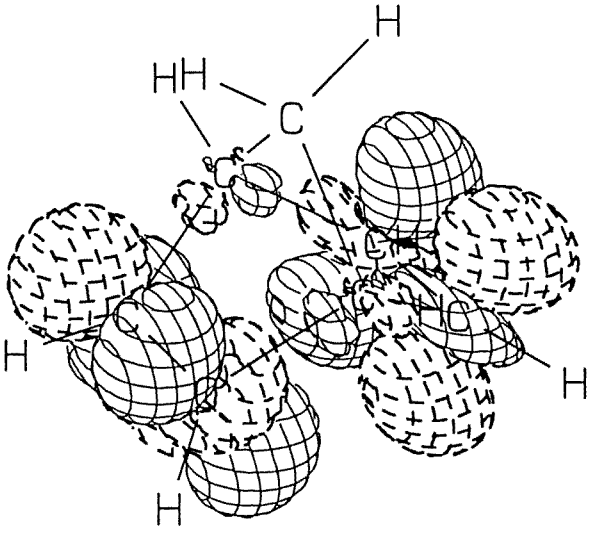

Fig. 6. Contour plot of the transition density, eq. (14), for the lowest singlet excitation in norbornadiene.

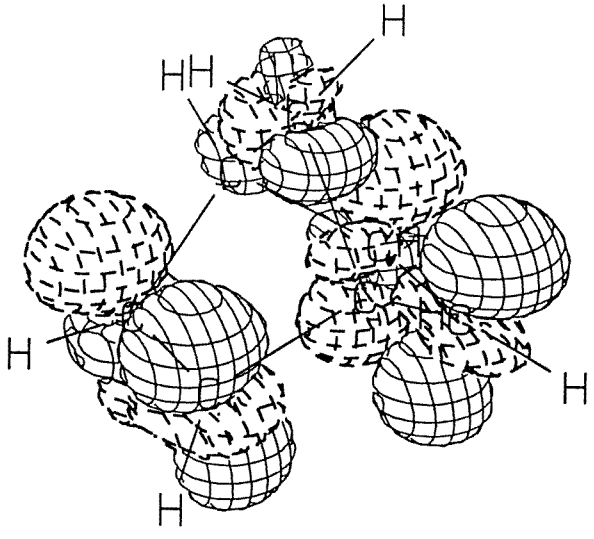

Fig. 7. Contour plot of the transition density, eq. (14), for the fourth singlet excitation in norbornadiene, on the same scale as fig. 6.

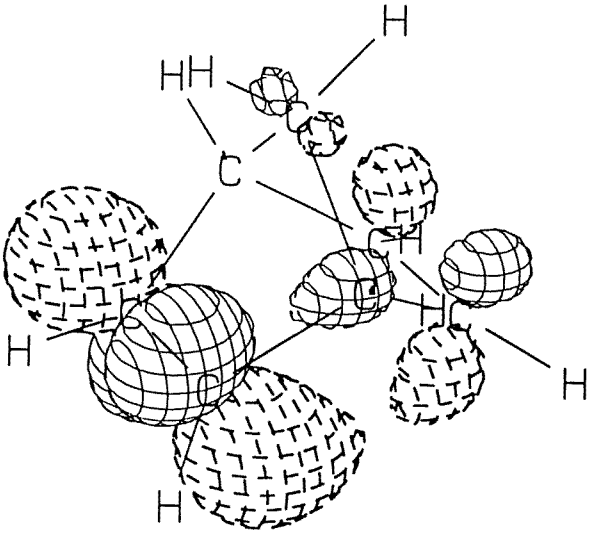

Fig. 8. Contour plot of localized EVO for half of the lowest excitation in norbornadiene.

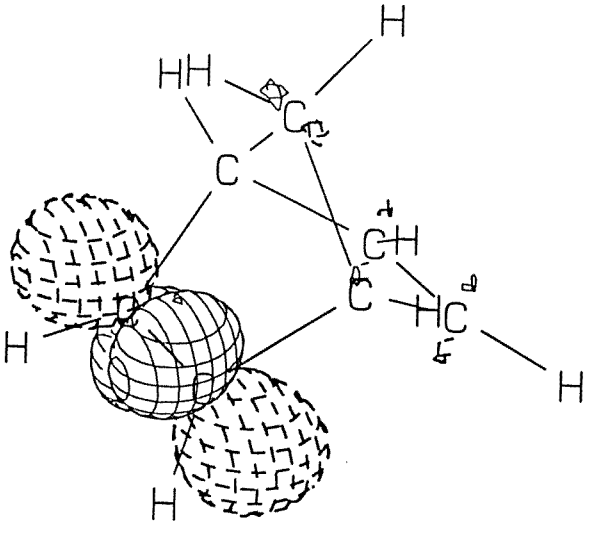

Fig. 9. Contour plot of localized EVO for half of the fourth excitation in norbornadiene, on the same scale as fig. 8.

in fig. 6, while the transition density in fig. 7 has a pronounced dipolar component, corresponding to the strongly allowed, y-polarized electric dipole intensity of this B_2 transition.

Figures 4–7 illustrate the overall properties of the transitions. To address the question of charge transfer between the two chromophoric groups, we show in figs. 8 and 9 the effective virtual orbitals (EVOs, eq. (25)), for excitation out of the localized $\pi(5, 6)$ orbital (see fig. 1) in the A_2 and the B_2 transitions, respectively. Note that fig. 6 is largely represented by the out-of-phase combination of the EVO in fig. 8 with its counterpart from the other chromophore, while fig. 7 is largely represented by the in-phase combination of the EVO in fig. 9 with its counterpart from the other chromophore. Figures 7 and 8 show that although both transitions are dominated by localized, i.e., exciton-like excitations, since the EVOs are concentrated in the 5–6 bond region, the EVO in fig. 8 nevertheless indicates considerable charge-transfer character for the A_2 transition, whereas charge transfer appears to play a much smaller role for the B_2 transition.

An attempt to quantify the degree of localization in these two transitions is represented by the values given in table 1 for the locally excited and charge-transfer characters, %LE and %CT, respectively. These represent the normalization contributions (on a percentage scale) according to eq. (9), obtained after transformation to a basis where the occupied orbitals are localized, and subsequently redelocalized within the chromophores (see section 2), and where one virtual orbital is localized relative to each bonding occupied orbital. This procedure generates local pairs of σ, σ^* orbitals for the molecular single bonds, and pairs of σ, σ^* and π, π^* orbitals in the two chromophores. %LE is then the sum of the normalization contributions from the two localized π–π^* excitations, whereas %CT is the sum of the normalization contributions from the two charge-transfer π–π^* excitations (excitations involving chromophoric σ and σ^* orbitals contribute less than 2%).

Hence, by this account the locally excited, i.e., the molecular exciton-like, contributions amount to about 50% of the total normalization of the excitation amplitudes for both transitions. However, interchromophoric charge-transfer amounts to 25% and 10% of the A_2 and the B_2 transitions, respectively. These values agree quite well with the degree of charge-transfer admixture apparent in figs. 8 and 9. If the non-conjugated diene moiety is considered an extended chromophore, the extrachromophoric normalization contributions to the A_2 transition amount to only about 20%, whereas the B_2 transition contains about 45% extrachromophoric character. This corroborates the difference in overall molecular involvement in the charge rearrangements in figs. 3 and 4 and the difference in $\Delta\langle r^2\rangle$ values for the two transitions.

To analyze the intensity contributions for the two valence transitions, and hence establish contact with the exciton coupling model, we show in table 2 the bond decompositions of the electric dipole transition moments in velocity form, as defined in eq. (17). Notice that the values given for the $\pi(5, 6)$ bond contributions represent the respective velocity transition moments for excitation out of this orbital

Table 2

Leading bond contributions to the electric dipole transition moment of the valence transitions in norbornadiene.

Bond (α)[a]	$P_{y\alpha}(A_2)$[b),c)]	$P_{y\alpha}(B_2)$[b),c)]
$\sigma(5, 6)$	0.001	0.013
$\pi(5, 6)$	−0.215	−0.206
$\sigma(2, 3)$	−0.001	0.013
$\pi(2, 3)$	0.215	−0.206
$\sigma(1, 7)$	0.000	0.030
$\sigma(4, 7)$	0.000	0.030
$\sigma(7, Ha)$	0.010	0.027
$\sigma(7, Hb)$	−0.010	0.027
Total	0.000	−0.255

[a] A "bond" is defined here as the localized molecular orbital connection the pair of atoms indicated.
[b] Bond contributions (a.u.) in the velocity form, eq. (17).
[c] Only the y-components are large.

into the EVOs given in figs. 8 and 9. This decomposition shows that the chromophoric contributions are of about the same magnitude in the two transitions, and enter with, respectively, out-of-phase and in-phase sign combinations. Both features are in accord with an exciton approach. However, the decomposition also shows that the overall transition moment of the B_2 excitation is reduced significantly from the inherent chromophoric value of about −0.390 to the resultant −0.255, corresponding to a "hypochromic" effect of about 40% from the oscillator strength predicted by the chromophoric moments alone to the value given in table 1. By the same token, transferability of the ab initio values for the inherent chromophoric transition moments is not supported by this difference in the importance of extrachromophoric contributions in the two transitions.

Turning briefly to the Rydberg-like transitions we note that, consistent with the symmetry of the valence transitions, only the A_2 and B_2 transitions calculated at 7.01 eV and 7.16 eV contain valence-like contamination, as measured by the locally excited and charge-transfer characters for these transitions. The latter are indeed valid (lower limit) indicators of valence contributions in the present case, since the σ^* and π^* orbitals generated when only one virtual orbital is localized relative to each bonding orbital are quite compact. This observation is consistent with the comment made earlier, that the single orbital promotions indicated as assignments for the Rydberg transitions in table 1 account for at least 70% of the normalization. In a chromophore context, the Rydberg orbitals are not particularly revealing, since they sample the entire molecule and their quantization is determined by the overall molecular skeleton, as shown in figs. 2 and 3. The same behavior

was also illustrated in our earlier work on mono-olefins [34], and on methyl-substituted 3-membered rings [35].

An assignment of the transitions, strictly speaking, involves all of the above results and comments. However, if forced to make a choice that will fit into the space allotted to the assignment in a table of results, we tend to favor the notation according to the exciton model employed for the valence transitions in table 1, since localization and exciton-like behavior appear to be the most well-developed features for these transitions. Canonical orbital assignments, on the other hand, clearly are most appropriate for the Rydberg transitions.

3.2. METHYLADAMANTANONE

The molecule 4(e)-methyladamantanone (EMAO), fig. 10, contains a carbonyl chromophore as part of a rigid cage made chiral by the equatorially-substituted methyl group at position 4. In the absence of the substituent the molecule shares

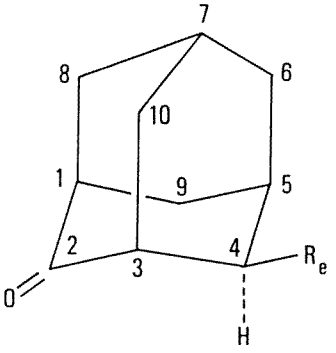

Fig. 10. Geometry and atom numbering in 4(e)-methyladamantanone (EMAO).

with the chromophore a C_{2v} point group symmetry, and the lowest spin-singlet transition, the $n \rightarrow \pi^* A_2$ excitation, is electric-dipole-forbidden–magnetic-dipole-allowed, with the magnetic dipole transition moment along the C=O axis. The symmetry lowering caused by the methyl group endows the erstwhile $n \rightarrow \pi^*$ excitation with a non-vanishing electric dipole transition moment, and hence with a non-vanishing circular dichroism (CD) as given by the rotatory strength, eq. (2).

In a phenomenological chromophore language, this system is a prime example of a molecule whose optical activity can be rationalized in terms of the concept of a symmetric chromophore perturbed by dissymmetrically disposed molecular surroundings [36]. For carbonyl-containing compounds, this concept has led to the so-called Octant Rule [37]. The rule divides all space surrounding the carbonyl group into eight regions (octants), and for a single substituent, the octant occupied

by that substituent determines the sign of the rotatory strength of the $n \rightarrow \pi^*$ transition. For a survey of the history of the octant rule and of the various detailed mechanisms studied over the years, see refs. [38,39]. In addition, the optical activity of saturated ketones exhibits a particularly intriguing feature of extrachromophoric perturbations/interactions, namely the importance of contributions that can be ascribed to so-called open zigzag lines [38,40]. In the present case, this translates into the expectation that contributions connected with bonds along a path such as $3-4-\gamma-ax$ (see fig. 11) should be particularly pronounced, implying a very specific molecular embedding effect.

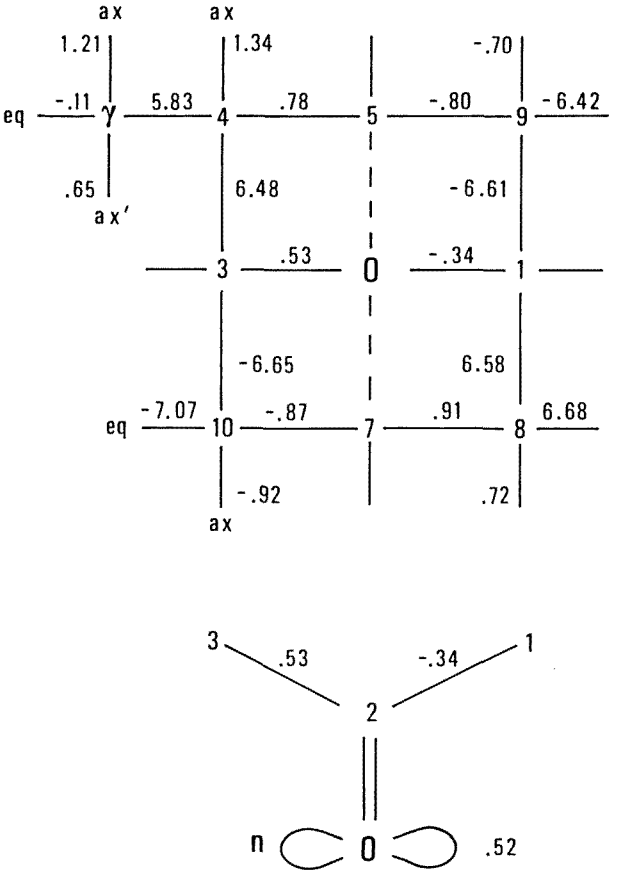

Fig. 11. Effective bond contributions to the $n \rightarrow \pi^*$ rotatory strength in EMAO.

References [38] and [39] present theoretical treatments of various prototypical octant rule ketones including EMAO; Rodger and Rodger [39] use an independent systems/perturbation approach, while ref. [38] presents a minimal-basis RPA calculation and an analysis of the circular dichroism along the lines of eqs. (22)–(24). The

above-mentioned open zigzag pattern was indeed found in the bond contributions extracted from the RPA results in ref. [38], and in ref. [40], Rodger and Moloney extend the idea of orbital-following [27,41] to argue that charge transfer between the carbonyl group and the surrounding molecule provides a qualitative rationale for the importance of bonds in open zigzag paths.

The methyladamantanone (EMAO) calculations presented here were performed on the Cray Y/MP machine at the National Center for Supercomputing Applications at the University of Illinois. The molecular orbitals were generated using the Gaussian 90 program [29], and the electronic excitation properties were computed with Program RPAC [30]. We used a force-field optimized (MM2) geometry [38], and the Dunning–Hay (3s2p) basis set [32], providing a total of 140 atomic orbitals. This basis set yielded a Hartree–Fock ground-state energy of −500.585530 hartrees, and generated 3135 singly-excited configurations out of the valence occupied orbitals. Again, the corresponding ca. 9,000,000 double excitations are included automatically through the **B** matrix. All configurations were included in the iterative solution of the RPA equations [30], and the overall results for the lowest excitation are included in table 3. As is commonly found in these calculations, the energy is somewhat

Table 3

Computed results for the lowest excitation in 4(e)-methyladamantanone (EMAO).

ΔE [eV]	$f^{r\nabla}$	$R^{a)}$	Intr$^{a),b)}$	μ–$m^{a),b)}$	μ–$\mu^{a),b)}$
Exp.$^{c)}$ 4.20	–	1.80			
Calc. 4.72	$<10^{-3}$	1.68	0.15	1.21	0.32
$n^{d)}$			0.12	0.75	0.01
$n'^{e)}$			−0.25	1.50	0.35

a) In units of 10^{-40} cgs.
b) The three contributions to eq. (22a).
c) From ref. [38].
d) The three contributions to eq. (22a) for α equal to the non-bonding orbital (see text).
e) The three contributions to eq. (22a) for α equal to the non-bonding orbital plus the bond orbitals 2–3 and 2–1 (see text).

overestimated, whereas the computed rotatory strength is of the right sign and magnitude. However, although this implies that the excitation has a non-vanishing electric dipole transition moment, its magnitude is so small that the resulting computed oscillator strength is less than 10^{-3}.

For the interpretation of the actual spectra, these intensity features imply in general that the "forbidden" components can be expected to dominate the band shape for the ordinary absorption spectrum of this type of ketone, while the magnitude of the rotatory strength is such that both "allowed" and "forbidden" components may contribute (sometimes with opposite signs) to the band shape of the circular

dichroism [3,13].* Table 3 accordingly contains no experimental value for the oscillator strength. The experimental value for the rotatory strength is estimated from the low temperature CD assuming that the allowed component dominates the band shape [38].

Turning now to the analysis of the calculated intensity, the decomposition of the overall rotatory strength into the three mechanistic contributions in eq. (22a), table 3, shows that the sign and magnitude is determined by the $\mu-m$ term, which corresponds to the coupling between local electric and magnetic dipole transition moments. The small size of the intrinsic contribution shows that the overall chiral structure of the molecule has not induced significant dissymmetry into the individual localized bond orbitals. In other words, the results do not support a model assigning the effect principally to a static perturbation exerted by the extrachromophoric parts of the molecule. The $\mu-\mu$ contribution, however, shows that the polarizability (or moment-of-momentum) interactions between the local electric dipole transition moments add constructively to the circular dichroism.

This table also contains two subsets of contributions corresponding to eq. (22a). In the row labeled n, all the terms represent couplings between the localized non-bonding orbital on the oxygen atom and all other bonds in the molecule, and in the row labeled n', all the terms represent couplings between the extended "non-bonding" system, i.e., the localized non-bonding orbital and the localized orbitals in bonds 2–3 and 2–1, and all other bonds in the molecule. As expected, the essential part of the overall $\mu-m$ mechanism thus comes from the coupling between the local magnetic dipole transition moment associated with the chromophore and electric dipole bond transition moments from the rest of the molecule.

In terms of the effective bond contributions, eq. (24), the prominence of the bonds in the open zigzag paths is quite apparent in fig. 11. The signs of the large bond contributions all conform to the prediction of the octant rule for the contribution to the CD from a perturbing substituent in the respective octants [3,38]. While the skeleton contributions largely cancel across the erstwhile symmetry planes, the additional contributions from the non-bonding orbital and from the methyl orbitals tip the balance to the overall resulting positive rotatory strength.

To analyze the mechanism in more detail, table 4 shows the absolute values of RPA amplitudes transformed to a basis in which one virtual orbital is localized relative to each bond orbital (in such a localization scheme there are no virtual orbitals localized relative to the non-bonding orbitals). Only absolute values are shown since the signs depend on the arbitrary phases of the individual orbitals. Apart from contributions within the chromophore itself, only bonds in zigzag paths are included, since the amplitudes for excitation out of or into orbitals localized in the other bonds all contribute less than 0.1% to the normalization. Local $\sigma \rightarrow \sigma^*$

* A word of caution for the chirally uninitiated: in addition to these vibronic considerations, the possible effects of solvation [39] and of equilibria between different molecular conformations [38] must be taken into account in the structural interpretation of weak circular spectra.

Table 4

Contributions from individual bonds and local excitations to $n \rightarrow \pi^*$ rotatory strength of EMAO.

		$\lvert X-Y \rvert$[a]			
Bond α[b]	$R_{\alpha,\mathrm{eff}}$[b),c)]	$\alpha \rightarrow \pi^*$	$n \rightarrow \alpha^*$	$(2-3) \rightarrow \alpha^*$	$(2-1) \rightarrow \alpha^*$
n	0.52	0.770	x[d)]	x	x
2–3	0.53	0.340	y[e)]	y	y
2–1	–0.34	0.337	y	y	y
3–4	6.48	0.066	0.121	0.050	0.050
4–γ	5.83	0.052	0.088	0.043	0.040
3–10	–6.65	0.066	0.121	0.054	0.050
10–eq	–7.07	0.052	0.092	0.044	0.042

[a] Numerical value of RPA amplitude.
[b] See figs. 10 and 11.
[c] Effective bond contributions in units of 10^{-40} cgs.
[d] There is no well-defined virtual orbital localized relative to the non-bonding orbital.
[e] These amplitudes contribute less than 0.1% to the normalization.

excitations in the individual bonds are seen to be of no importance, whereas it is apparent that both charge transfer from these bonds into the localized π^* carbonyl orbital and from the "extended" non-bonding carbonyl orbital system into the localized antibonding orbitals in the bonds play a role. Here, the charge transfer out of the non-bonding orbital contributes mainly to the magnetic dipole transition moment, whereas charge transfer into the π^* orbital contributes mainly to the electric dipole transition moment. We therefore agree with Rodger and Moloney [40] that in general terms charge transfer seems to be the essential ingredient in enhancing rotatory strength contributions associated with bonds in the open zigzag paths. The amplitudes given in table 4 provide an illustrative quantification of this effect.

In the present context, this molecule therefore provides a case where the chromophore, as defined in terms of the dominating excitation amplitudes and hence spectral location of the transition energy, can be clearly identified with the carbonyl group, since more than 80% of the normalization comes from excitations from the extended non-bonding system into the localized π^* orbital. On the other hand, from the point of view of the circular dichroic intensity the chromophoric part of the molecule must be redefined to include bonds in the open zigzag paths. The importance of charge transfer (i.e., delocalization in a general sense) furthermore implies that the electric dipole bond moments, which are extracted via eqs. (16) and (17) and employed in the mechanistic analysis, are specific to this extended chromophore and hence cannot be treated as transferable quantities.

4. Concluding remarks

We have demonstrated how the invariance of the Random Phase Approximation with respect to transformations between canonical and non-canonical molecular orbital bases allows one to analyze the results of an ab initio calculation of the electronic transitions in a given molecule either in terms of a delocalized, symmetry-characteristic description or in terms of a localized, bond-characteristic description. For the specific molecules considered here, the delocalized description is the natural choice for the assignment of the Rydberg transitions, whereas the localized description is appropriate for the desired investigation of the chromophore aspect of the valence transitions. For the latter purpose, we defined a number of bond-characteristic quantities, notably normalization contributions, eq. (15), bond transition moments, eqs. (6)–(18), and effective virtual orbitals, eq. (25); the bond moments in turn provide the decompositions of the overall intensities in eqs. (21)–(24).

Based on these various measures of localized contributions, we have presented a two-layered analysis of the lowest valence transitions in norbornadiene (NBD), showing (i) to what extent the non-diene parts of the molecule participate in the excitations, and (ii) to what extent a molecular exciton model is justified for this non-conjugated diene chromophore. For the chiral methyladamantanone molecule (EMAO), we analyzed the mechanism and localized contributions for the CD intensity of the lowest, erstwhile $n \rightarrow \pi^*$, transition, and showed that charge transfer between the carbonyl group and bonds in the characteristic open zigzag paths plays a dominating role; or in other words that the chromophore for the circular dichroic intensity of this transition effectively extends throughout the molecule.

These analyses have therefore definitely identified the fragments of the molecules that can be considered the chromophores, and have shown the importance of the distinction between the fragment that bears the primary responsibility for the location of the spectral line and the fragment that determined the intensity. Whether the environmental effects on the intensity are considered as perturbations due to molecular embedding, i.e., an auxochromic effect [1], or as evidence of an extended chromophore, is to some extent a matter of taste. In view of the importance of charge transfer in the intensity mechanisms, we tend to favor the latter view.

At the same time, these analyses show that the various localized contributions, especially the bond moments, are quite specific to the particular overall electronic excitation from which they are extracted, and also quite sensitive to the extrachromophoric parts of the molecules. They cannot, therefore, be expected to be transferable in general. A striking example of this is the electric dipole bond moments contributing to the rotatory strength of the $n \rightarrow \pi^*$ transition in EMAO, which are totally dominated by charge transfer out of the bonds to which these moments are formally assigned.

It should be emphasized that the present analyses are directed towards decomposing intensity-related quantities. We have made no attempt to correlate the

energetics of the excitations with the energetic aspects of the exciton coupling model [1] or of the more general dynamic coupling models [3,39]; such a correlation is beyond the scope of the present work.

Acknowledgements

Aa.E.H. is grateful to Dr. Ruth McDiarmid for a helpful discussion regarding the experimental assignments of NBD, and to Dr. Alison Rodger for a preprint of ref. [40]. T.D.B. acknowledges support from the US National Science Foundation (Grant No. CHe-9007809) and an allocation of computer time at the National Center for Supercomputing Applications. We thank Dr. Robert Kirby for a critical reading of the manuscript.

References

[1] J.N. Murrell, *The Theory of the Electronic Spectra of Organic Molecules* (Methuen, London, 1963).
[2] P. Jørgensen and J. Simons, *Second Quantization-Based Methods in Quantum Chemistry* (Academic Press, New York, 1981).
[3] Aa.E. Hansen and T.D. Bouman, Natural chiroptical spectroscopy: Theory and computations, Adv. Chem. Phys. 44(1980)545.
[4] T.D. Bouman and Aa.E. Hansen, Ab initio calculations and mechanistic analyses of optical activity of organic molecules with extended chromophores, Croat. Chim. Acta 62(1989)227.
[5] T.D. Bouman and Aa.E. Hansen, Linear response calculations of molecular properties using program RPAC: NMR shielding tensors of pyridine and *n*-azines, Int. J. Quant. Chem. Quant. Chem. Symp. 23(1989)381.
[6] O. Chalvet et al. (eds.), *Localization and Delocalization in Quantum Chemistry*, Vols. 1 and 2 (Reidel, Dordrecht, 1976).
[7] P.R. Surján, Interaction of chemical bonds: Strictly localized wave functions in orthogonal basis, Phys. Rev. A30(1984)43 and later papers.
[8] A.E. Reed and F. Weinhold, Natural localized molecular orbitals, J. Chem. Phys. 83(1985)1736 and later papers.
[9] B. Kirtman, Molecular electronic structure by combination of fragments, J. Phys. Chem. 86(1982)1059 and later papers, as reviewed in C.E. Dykstra and B. Kirtman, Local quantum chemistry, Ann. Rev. Phys. Chem. 41(1991)155–174.
[10] D.E. LaLonde, J.D. Petke and G.M. Maggiora, Evaluation of approximations in molecular exciton theory, Part 1. Applications to dimeric systems of interest in photosynthesis, J. Phys. Chem. 92(1988)4746; Part 2. Applications to oligomeric systems of interest in photosynthesis 93(1988)608.
[11] J.D. Petke, Construction of chromophore orbitals, J. Chem. Phys. 93(1990)2561.
[12] P. Pulay, Localizability of dynamic electron correlation, Chem. Phys. Lett. 100(1983)151 and later papers.
[13] C.J. Ballhausen and Aa.E. Hansen, Electronic spectra, Ann. Rev. Phys. Chem. 23(1972)15.
[14] Aa.E. Hansen and T.D. Bouman, Hypervirial relations as constraints in calculations of electronic excitation properties: The random phase approximation in configuration interaction language, Mol. Phys. 37(1979)1713.
[15] J. Oddershede, P. Jørgensen and D.L. Yeager, Polarization propagator methods in atomic and molecular calculations, Comp. Phys. Rep. 2(1984)33.

[16] T.D. Bouman, B. Voigt and Aa.E. Hansen, Optical activity of saturated ketones: Ab initio localized orbital analysis of a model ketone in the random phase approximation, J. Amer. Chem. Soc. 101(1979)550.

[17] D. Lynch, M.F. Herman and D.L. Yeager, Excited state properties from the equations of motion method. Application of the MCTDHF-MCRPA to the dipole moments and oscillator strengths of the $A^1\Pi$, $a^3\Pi$, $a'^3\Sigma^+$, and $d^3\Delta$ low-lying valence states of CO, Chem. Phys. 64(1982)69.

[18] Aa.E. Hansen and T.D. Bouman, Optical activity of mono-olefins: RPA calculations and extraction of the mechanisms in Kirkwood's theory. Application to (–)-*trans*-cyclooctene and 3(*R*)-methylcyclopentene, J. Amer. Chem. Soc. 107(1985)4828.

[19] J.M. Foster and S.F. Boys, Canonical configuration interaction procedure, Rev. Mod. Phys. 32(1960)300.

[20] T.D. Bouman, Aa.E. Hansen, B. Voigt and S. Rettrup, Large-scale RPA calculations of chiroptical properties of organic molecules: Program RPAC, Int. J. Quant. Chem. 23 (1983)595.

[21] J.G. Kirkwood, On the theory of optical rotatory power, J. Chem. Phys. 5(1937)479; Remarks on the theory of optical activity, J. Chem. Phys. 7(1939)139.

[22] J.A. Schellman, Symmetry rules for optical rotation, Acc. Chem. Res. 1(1968)144.

[23] J. Olsen, H.J.Aa. Jensen and P. Jørgensen, Solution of the large matrix equations which occur in response theory, J. Comp. Phys. 74(1988)265.

[24] J.P. Doering and R. McDiarmid, An electron impact investigation of the forbidden and allowed transitions in norbornadiene, J. Chem. Phys. 75(1981)87.

[25] D.A. Lightner, J.K. Gawroński and T.D. Bouman, Electronic structure of symmetric homoconjugated dienes: Circular dichroism of (1S)-2-deuterio- and 2-methylnorbornadiene and (1S)-2-deuterio and 2-methylbicyclo[2.2.2]octadiene, J. Amer. Chem. Soc. 102(1980)5749.

[26] C.F. Wilcox, Jr., S. Winstein and W.G. McMillan, Neighboring carbon and hydrogen, 34. Interaction of non-conjugated chromophores, J. Amer. Chem. Soc. 82(1960)5450.

[27] R. Hoffmann, Interaction of orbitals through bonds and through spaces, Acc. Chem. Res. 4(1971)1.

[28] V. Galasso, Ab initio calculations on the one-photon and two-photon electronic transitions of cyclopentadiene, spirononatetraene, 1,4-cyclohexadiene, Dewar benzene, norbornadiene, and barrelene, Chem. Phys. 153(1991)13.

[29] M.J. Frisch, M. Head-Gordon, G.W. Trucks, J.B. Foresman, H.B. Schlegel, K. Raghavachari, M.A. Robb, J.S. Binkley, C. Gonzalez, D.J. Defrees, D.J. Fox, R.A. Whiteside, R. Seeger, C.F. Melius, J. Baker, R.L. Martin, L.R. Kahn, J.J.P. Stewart, S. Topiol and J.A. Pople, Gaussian 90 (Gaussian, Inc., Pittsburgh, PA, 1990).

[30] T.D. Bouman and Aa.E. Hansen, *RPAC Molecular Properties Package, Version 9.0X* (Southern Illinois University at Edwardsville, 1991).

[31] K. Gilbert and J. Gajewski, *Program PCMODEL* (Serena Software, P.O. Box 3076, Bloomington, IN 47402).

[32] T. Dunning and J. Hay, Gaussian basis sets for molecular calculations, in: *Methods of Electronic Structure Theory*, Vol. 3, ed. H.F. Schaefer III (Plenum, New York, 1977).

[33] W.L. Jorgensen and L. Salem, *The Organic Chemist's Book of Orbitals* (Academic Press, New York, 1973);
H. Morrison, W.L. Jorgensen, B. Bigot, D. Severance, Y. Munoz-Sola, R. Strommen and B. Pandey, Delta plots – a new way to visualize electronic excitation, J. Chem. Educ. 62(1985)298.

[34] T.D. Bouman and Aa.E. Hansen, Electronic spectra of mono-olefins. RPA calculations on ethylene, propene, and *cis* and *trans*-2-butene, Chem. Phys. Lett. 117(1985)461.

[35] S. Bohan and T.D. Bouman, RPA calculations and analysis of the electronic states of cyclopropane and of the chiroptical properties of its methyl derivatives, J. Amer. Chem. Soc. 108(1986)3261.

[36] A. Moscowitz, Some applications of the Kronig–Kramers theorem to optical activity, Tetrahedron 13(1961)48;
A. Moscowitz, Theoretical aspects of optical activity, Part 1: Small molecules, Adv. Chem. Phys. 4(1962)67.

[37] W. Moffitt, R.B. Woodward, A. Moscowitz, W. Klyne and C. Djerassi, Structure and optical rotatory dispersion of saturated ketones, J. Amer. Chem. Soc. 83(1961)4013.

[38] D.A. Lightner, T.D. Bouman, W.M.D. Wijekoon and Aa.E. Hansen, Mechanism of ketone $n \rightarrow \pi^*$ optical activity. Experimental and computed chiroptical properties of 4-axial and 4-equatorial alkyladamantanones, J. Amer. Chem. Soc. 108(1986)4484.

[39] A. Rodger and P.M. Rodger, The circular dichroism of the carbonyl $n \rightarrow \pi^*$ transition: An independent systems/perturbation approach, J. Amer. Chem. Soc. 110(1988)2361.

[40] A. Rodger and M.G. Moloney, $n \rightarrow \pi^*$ circular dichroism of planar zigzag carbonyl compounds, J. Chem. Soc. Perkin Trans. II(1991)919.

[41] C.C. Levin, R. Hoffmann, W.J. Hehre and J. Hudec, Orbital interactions in amino-ketones, J. Chem. Soc. Perkin Trans. II(1973)210.